

Towards the centrality dependence description of the charge balance function in the HYDJET++ model

A.S. Chernyshov¹, G.Kh. Eyyubova¹, V.L. Korotkikh¹, I.P. Lokhtin¹,
L.V. Malinina¹, S.V. Petrushanko¹, A.M. Snigirev^{1,2}, and E.E. Zabrodin^{1,3}

¹ *Skobeltsyn Institute of Nuclear Physics, Lomonosov Moscow State University, RU-119991 Moscow, Russia*

² *Bogoliubov Laboratory of Theoretical Physics, JINR, RU-141980 Dubna, Russia and*

³ *Department of Physics, University of Oslo, N-0316 Oslo, Norway*

Data from the Large Hadron Collider on the charge balance function in Pb+Pb collisions at center-of-mass energy 2.76 TeV per nucleon pair are analyzed and interpreted within the framework of the HYDJET++ model. This model allows us to reproduce the experimentally observed centrality dependence of the balance function widths at the relatively low transverse momentum intervals qualitatively due to the different charge creation mechanisms in soft and hard processes. However, the fully adequate description of the balance function in these intervals implies the essential model modification by including the exact charge conservation in terms of the canonical ensemble instead of the grand canonical one. A procedure is proposed for introducing charge correlations into the thermal model without changing other model parameters. With increasing transverse momenta, the default model results describe experimental data much better because the contribution from the soft component of the model is significantly reduced in these transverse momentum intervals. In practice, there is a transition to a single source of charge correlations, namely, charge correlations in jets for which the exact charge conservation takes place at each stage.

PACS numbers: 25.75.-q, 24.10.Nz, 24.10.Pa

I. INTRODUCTION

With the Relativistic Heavy Ion Collider (RHIC) and the Large Hadron Collider (LHC) in operation one can access a number of exquisite and intriguing phenomena which could have never been systematically studied at previous generation of the accelerators. The anisotropic flow, the energy loss of high transverse momentum particles, the charge balance function are among them as a sensitive probe of collective properties of a new state of matter, quark-gluon plasma (QGP); see, e.g., [1, 2]. The large number of these physical observables measured in heavy-ion collisions during RHIC and LHC operation can be successfully described within the framework of the popular HYDJET++ model [3]. For instance, the model calculations, such as transverse momentum spectra, pseudorapidity and centrality dependence of inclusive charged particle multiplicity and $\pi^\pm\pi^\pm$ correlation radii in central Pb+Pb collisions [4], centrality and momentum dependence of second and higher-order harmonic coefficients [5], flow fluctuations [6], jet quenching effects [7, 8], and angular dihadron correlations [9] are in fair agreement with the experimental data.

Some of the experimental measurements proposed as indicators of the QGP creation involve implicit understanding of quark production dependence on time. While, for example, the fact of strangeness enhancement has been well established indeed, it remains unclear whether the arbitrary mechanism is dominant during early ($\tau < 1$ fm/c) or late stages of the QGP fireball expansion. Charge balance function (CBF) was proposed in [10] as a mean for pinpointing the quark production in time by quantifying the separation of balancing charges. Connections between the CBFs, charge fluctuations and

correlations were discussed in [11], whereas in [12] it was shown that there was a possibility for specie binned CBFs to be applied as constraints of the diffusivity. Emergence of the charge balance functions was studied, e.g., in hydrodynamics [13], in thermal model with resonances [14], in coalescence model [15], as well as in other dynamic and statistical models [16]. Experimentally, charge balance function has been measured at RHIC [17–19] in pp, d+Au, and Au+Au collisions and at LHC [20–22] in pp, p+Pb, and Pb+Pb collisions. Charge balance function dependence on the collision centrality and beam energy are presented in these studies alongside some experimental techniques. An extensive overview of the CBF from both theoretical and experimental perspectives can be found in [23]. In the present paper we focus on the charge balance function as a provider of valuable insight into the charge creation mechanism as well.

The width of the balance function reported by the STAR Collaboration in [17] and by the ALICE Collaboration in [21] decreases with increasing centrality of the collisions. This centrality dependence is not reproduced by many event generators, e.g., HIJING [24, 25] and AMPT [26–28], and is a challenge for HYDJET++ also since the majority of soft particles is produced in the grand canonical ensemble approach where the charge conservation takes place in mean only. Nevertheless, the reasonable simple modification of the current version of the HYDJET++ model allows us to reproduce the experimentally observed nontrivial centrality dependence of the balance function widths qualitatively due to the different charge creation mechanisms in soft and hard processes. The further essential modernization is also suggested within the canonical ensemble approach to describe the charge balance function quantitatively.

The paper is organized as follows. Basic characteristics of the model are sketched in Sec. II. Section III presents the comparison of model results calculated within the default version of HYDJET++ with the experimental data. The widths of the CBFs in the model are broader compared to the experimental ones. Possible variation of the partial contributions of soft and hard processes to the CBFs are studied. The modification procedure that takes into account exact charge conservation in a single event without changing its bulk characteristics is introduced in Sec. IV. Implementation of this procedure in the HYDJET++ allows us to reproduce both widths and centrality dependence of the charge balance functions fairly well compared to the data. Conclusions are drawn in Sec. V.

II. HYDJET++ MODEL

It should be noted that currently there are many competing Monte Carlo event generators successfully describing the soft and hard momentum components of particle production in ultrarelativistic nuclear collisions separately. The HYDJET++ model belongs to the few ones, such as EPOS [29], QGSJET [30], PACIAE [31, 32], ANGAN-TYR [33], which aim to treat the soft and hard physics of the collisions simultaneously. For instance, the presence of both soft and hard processes “in one package” allows the model to reproduce recently [34] the experimentally observed [35] nontrivial centrality dependence of elliptic flow correlations at low and high transverse momenta in Pb+Pb collisions at LHC energies. The origin of the correlations between the low and high- p_T flow components in (semi)peripheral Pb+Pb collisions was traced to the correlations of particles in jets. As we will see below, these correlations are also important for the description of the charge balance function. Details of the model can be found in the HYDJET++ manual [3]. Here we stress and recall briefly the main features crucial for the present study only.

The HYDJET++ is a Monte Carlo event generator for simulation of relativistic heavy-ion collisions considered as a superposition of two independent components, namely, the soft hydro-type state and the hard state arising from the in-medium multiparton fragmentation. It is based on the adapted version of the event generator FASTMC [36, 37] and the PYQUEN partonic energy loss model [38].

In the hard part the partons are propagating through the expanding quark-gluon plasma and lose the energy due to parton rescattering and gluon radiation. The number of jets is generated in accordance with a binomial distribution. The mean number of jets produced in an A+A event is a product of the number of nucleon-nucleon (NN) binary subcollisions at a given impact parameter b and the integral cross section of the hard subprocess in these subcollisions with the minimum transverse momentum transfer p_T^{\min} . Its value is one of the input key

parameters of the model, because partons produced in (semi)hard processes with the momentum transfer lower than p_T^{\min} are excluded from the hard processes treatment. Their hadronization products are automatically added to the soft component of the particle spectrum.

The soft part of the model is represented by the thermalized hadronic state generated on the chemical and thermal freeze-out hypersurfaces prescribed by the parametrization of relativistic hydrodynamics with preset freeze-out conditions. Particle multiplicities are calculated within the effective thermal volume using a statistical model approach. The effective volume absorbs the collective velocity profile and the hypersurface shape. It is canceled out in all particle number ratios. Therefore, the latter do not depend on the freeze-out details as long as the local thermodynamic parameters are independent of spatial coordinates [36, 37]. The concept of the effective volume is applied to calculate the hadronic composition at both chemical and thermal freeze-outs. The number of particles in an event is calculated according to Poisson distribution around its mean value, which is supposed to be proportional to the number of participating nucleons for a given impact parameter of A+A collision. To simulate the elliptic and triangular flow effects, the hydro-inspired parametrization [39] for the momentum and spatial anisotropy of soft hadron emission source is implemented; see [3, 40, 41] for the details. In the following we refer to HYDJET++ version 2.4, freely available for download at [42], as the default version.

III. CBF AND CONTRIBUTIONS FROM SOFT AND HARD PROCESSES

The charge balance function has been proposed as a convenient measure of the resulting correlation between the oppositely charged particles [10]. It provides a valuable insight into the charge creation mechanism and can address the fundamental question concerning the hadronization process in nuclear collisions at relativistic energies. The final degree of correlations is reflected in the balance function and consequently in its width. It is defined as

$$B(\Delta\eta) = \frac{1}{2} \left[\frac{\langle N_{+-}(\Delta\eta) \rangle - \langle N_{++}(\Delta\eta) \rangle}{\langle N_+ \rangle} + \frac{\langle N_{-+}(\Delta\eta) \rangle - \langle N_{--}(\Delta\eta) \rangle}{\langle N_- \rangle} \right], \quad (1)$$

where $\langle N_{+-}(\Delta\eta) \rangle$ is the average number of opposite-charge pairs with particles separated by the relative pseudorapidity $\Delta\eta = \eta_+ - \eta_-$, similarly for $\langle N_{-+}(\Delta\eta) \rangle$, $\langle N_{++}(\Delta\eta) \rangle$ and $\langle N_{--}(\Delta\eta) \rangle$. Both particles of the pair have to fall into a certain pseudorapidity interval, for instance, $|\eta| < 0.8$ in accordance to the ALICE analysis conditions [21]. $\langle N_+ \rangle$ (and $\langle N_- \rangle$) is the number of positive (negative) charge particles in the pseudorapidity interval $|\eta| < 0.8$ averaged over all events. The charge

balance function $B(\Delta\varphi)$ as a function of the relative azimuthal angle $\Delta\varphi$ is defined in a similar way. Each term $N(\Delta\eta)$ is corrected for the acceptance limitation, reflecting the fact that the number of pairs in the limited acceptance has a maximum at $\Delta\eta = 0$.

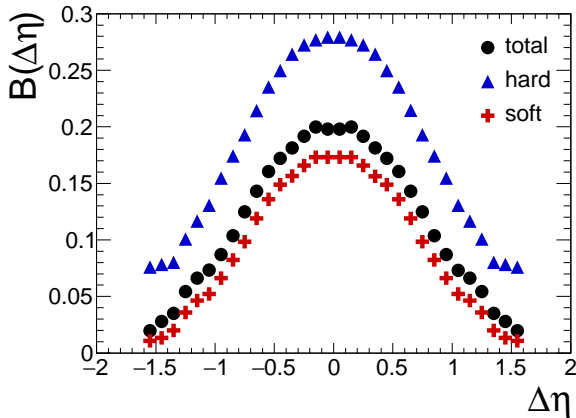


FIG. 1. (Color online) Balance function as a function of $\Delta\eta$ in Pb+Pb collisions at $\sqrt{s_{NN}} = 2.76$ TeV with centrality 0-5% calculated in HYDJET++ for each component, soft (crosses) and hard (triangles), together with the resulting total value (circles).

The width of the balance function distribution is defined as

$$\langle \Delta\eta \rangle = \frac{\sum_{i=1}^k [B(\Delta\eta_i) \cdot \Delta\eta_i]}{\sum_{i=1}^k B(\Delta\eta_i)}, \quad (2)$$

where $B(\Delta\eta_i)$ is the balance function value for each bin $\Delta\eta_i$ with the sum running over all bins k .

Figure 1 shows the charge balance function in terms of the pseudorapidity $\Delta\eta$ calculated in the HYDJET++ model separately for each component, soft and hard, together with the resulting total value. Calculations are done for Pb+Pb collisions at center-of-mass energy per nucleon pair $\sqrt{s_{NN}} = 2.76$ TeV with centrality 0-5%. One can see that the resulting total balance function is mainly dominated by the balance function of the soft component. It is not surprising, because in the momentum range $0.3 < p_T < 1.5$ GeV/c chosen for ALICE analysis [21] the majority of particles is soft. It is worth noting that the balance function of the soft component has been already studied [43] in the framework of the FASTMC event generator [36, 37] and has been compared to the STAR measurements [18]. The main results and conclusions of this study are the following.

In the statistical model, directly produced particles, called ‘‘primordial’’, are generated independently, and there are no balancing charge correlations. As a result, the FASTMC balance function vanishes for the ‘‘primordial’’ particles. In this approach, the phase-space correlations between the final state particles arise only from

the decays of hadronic resonances. Therefore, these correlations are determined merely by the kinematics of the decays. All charged particles falling into the considered pseudorapidity interval contribute to the denominator of Eq.(1), whereas only those from the resonance decays, i.e., correlated pairs, contribute to the numerator when one calculates the balance function for the soft component. At RHIC energies, for instance, about a quarter of the observed pions at the freeze-out are the ‘‘primordial’’ ones, while the other three quarters are produced via the resonance decays.

The balance functions for the soft component in terms of relative pseudorapidity, $\Delta\eta$, depend on the maximum transverse flow velocity and the thermal freeze-out temperature. The option with the large transverse flow and low thermal freeze-out temperature generally produces relatively smaller width of the balance function, compared to the higher thermal freeze-out temperature option. The width of the balance function is inversely proportional to the strength of the transverse flow. The balance functions calculated in the framework of the FASTMC generator are usually lower than those measured in central Au+Au collisions at center-of-mass energy 200 GeV per nucleon pair [43], indicating that there are another sources for charge correlations besides resonance decays. However, the widths of FASTMC balance function are rather close to those measured in central Au+Au collisions, indicating that an important source of the correlation between the opposite-charge particles is the decay of resonances.

The balance function in Fig. 1 for the soft hadrons coming from the hard component (for $0.3 < p_T < 1.5$ GeV/c) is higher than that for the soft component and its width is broader than the width of the soft component. This means that the charge correlations of the jet particles are weaker than those from the decay of resonances. It can be explained by the fact that the number of parton decays in the parton cascade during the jet fragmentation is larger than the number of consecutive resonance decays. Each subsequent decay makes the charge correlations weaker. The visible difference between the widths of soft and hard components opens some room to reproduce effectively the experimentally observed centrality dependence of the balance function widths. As a matter of fact, at the default parameters of HYDJET++ model the widths of the balance function do not reveal practically any centrality dependence, as shown in Fig. 2. The widths are calculated in the entire interval where the balance function is measured, i.e., $|\Delta\eta| < 1.6$ and $-\pi/2 < \Delta\varphi < 3\pi/2$. The applicability of the HYDJET++ generator for very peripheral collisions with centrality greater than 60% is doubtful due to a number of physical assumptions and approximations made in the model.

The centrality independence of the default model calculations indicates that some enhancement of the relative contribution from the jet part to the balance function is needed to reproduce the experimentally observed increase of the balance function widths in peripheral

Pb+Pb collisions. Actually, the mean “soft” and “hard” multiplicities depend on the centrality in different ways. They are roughly proportional to the mean number of participant nucleons $\langle N_{\text{part}}(b) \rangle$ and the mean number of binary NN subcollisions $\langle N_{\text{bin}}(b) \rangle$ at a given impact parameter b , respectively. The relative contribution of the soft and the hard parts to the total event multiplicity is fixed through the centrality dependence of the pseudorapidity hadron spectra $dN/d\eta$. The corresponding contribution from hydro and jet parts are mainly determined by the two input parameters: μ_{π}^{effth} , which is the (effective) chemical potential of positively charged pions at thermal freeze-out, and the minimum transverse momentum transfer of hard parton-parton scattering, p_T^{min} .

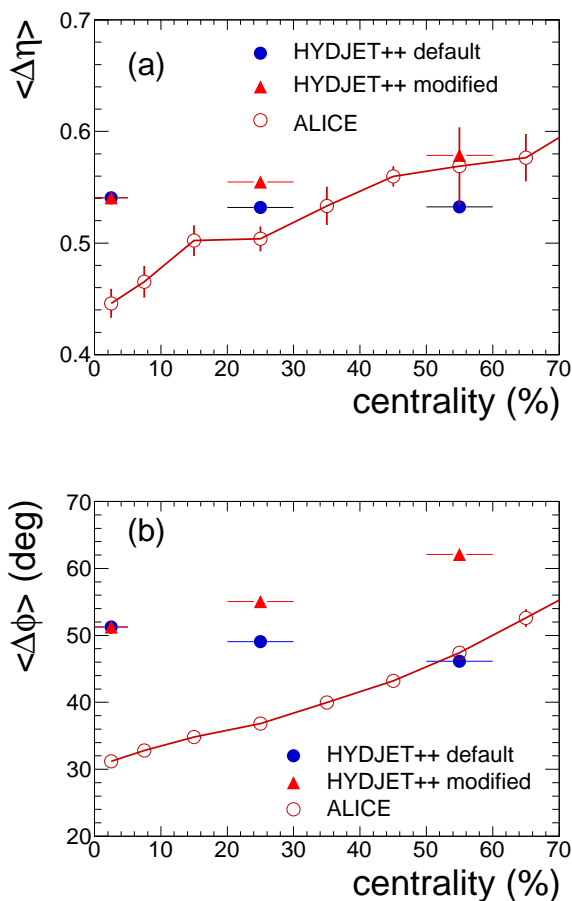


FIG. 2. (Color online) Centrality dependence of the width of the balance function of charged hadrons in Pb+Pb collisions at $\sqrt{s_{NN}} = 2.76$ TeV for the correlations studied in terms of (a) relative pseudorapidity $\langle \Delta\eta \rangle$ and (b) relative angle $\langle \Delta\phi \rangle$, respectively. The model calculations with default (full circles) and modified (triangles) versions of HYDJET++ are compared to the ALICE data (open circles) from [21]. Lines are drawn to guide the eye.

Besides, with the enhancement of the hard part for more peripheral collisions we decrease the contribution of

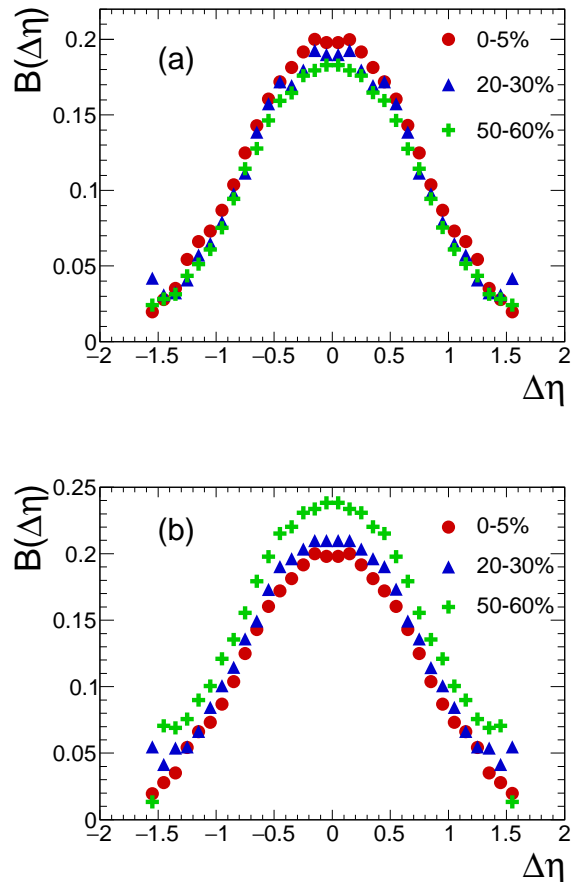


FIG. 3. (Color online) Balance function $B(\Delta\eta)$ of charged hadrons in Pb+Pb collisions at $\sqrt{s_{NN}} = 2.76$ TeV calculated within (a) HYDJET++ with the default parameters and (b) HYDJET++ with increased hard part and decreased soft part for three centralities, 0–5% (circles), 20–30% (triangles), and 50–60% (crosses).

TABLE I. Parameters of modified version of HYDJET++. See text for details.

Centrality	p_T^{min} , GeV/c	f_s
0-5%	8.2	1
20-30%	6.7	0.75
50-60%	5.15	0.395

soft component. As mentioned above, the contribution of the soft part to the total multiplicity changes with centrality because of its dependence on $\langle N_{\text{part}}(b) \rangle$. We additionally decrease it by the factor f_s . The values of p_T^{min} and f_s , listed in Table I, are adjusted in such a way that the total spectra dN/dp_T remain similar to that calculated with the default parameters $p_T^{\text{min}} = 8.2$ GeV/c and $f_s = 1$ for the given centrality.

The widths for the modified version show the desir-

able centrality dependence. However, our calculations are systematically higher than the experimental data. Moreover, the amplitudes of the modified balance functions shown in Fig. 3 demonstrate the opposite centrality dependence compared to the default model calculations. These amplitudes become larger with increasing impact parameter for calculations within the modified version unlike the default model results, for which the amplitudes are reduced in accord to the experimental data [21]. This discrepancy requires explanation. In HYDJET++ model we have two independent sources of charge correlations, namely, the resonances with the width $\langle\Delta\eta\rangle_{\text{res}}$ and the jets with $\langle\Delta\eta\rangle_{\text{jet}}$. Note that $\langle\Delta\eta\rangle_{\text{res}}$ is less than $\langle\Delta\eta\rangle_{\text{jet}}$. The resulting width has a some intermediate value between $\langle\Delta\eta\rangle_{\text{res}}$ and $\langle\Delta\eta\rangle_{\text{jet}}$ depending on the relative contribution from these sources. The widths $\langle\Delta\eta\rangle_{\text{res}}$ and $\langle\Delta\eta\rangle_{\text{jet}}$ are initially larger than $\langle\Delta\eta\rangle_{\text{exp}}$, therefore, any resulting width from these sources will be larger than $\langle\Delta\eta\rangle_{\text{exp}}$ also. Our observation indicates that some additional source of the charge correlation with the width less than $\langle\Delta\eta\rangle_{\text{res}}$ is needed to reproduce experimentally observed one in the considered interval of relatively low transverse momenta.

For higher transverse momentum regions it was found [20] that the balance function is getting narrower thus indicating that the correlations become stronger. Moreover, the centrality dependence of the widths practically vanishes. We compare the widths calculated at the high transverse momenta in the intervals

- (1) $2.0 < p_{T,\text{assoc}} < 3.0 < p_{T,\text{trig}} < 4.0$ GeV/c and
- (2) $3.0 < p_{T,\text{assoc}} < 8.0 < p_{T,\text{trig}} < 15.0$ GeV/c

with the data [20]. Here the widths were calculated in accordance with experimental calculation not in the entire intervals of $\Delta\eta$, $\Delta\phi$, but in the narrow interval. The balance function distributions are fitted to a sum of a Gaussian and a constant. The width is then calculated within $3\sigma_{\text{Gauss}}$. The comparison is displayed in Fig. 4. One can see in this figure that with increasing transverse momentum the default model results describe the experimental data much better since in these transverse momentum intervals the contribution from the soft component becomes weaker. Practically we observe the transition to the single source of charge correlations, namely, the charge correlations in jets for which the exact charge conservation takes place at each stage. The decrease of the width with increasing transverse momentum can be explained also. Namely, particles with higher transverse momenta are created closer to the beginning of parton cascade, where the charge correlations are stronger.

IV. IMPLEMENTATION OF EXACT CHARGE CONSERVATION IN THE MODEL

Our investigation reveals that the interval of relatively low transverse momenta remains problematic in description of the charge balance function despite the attempts made. This is a long-standing conceptual problem. The

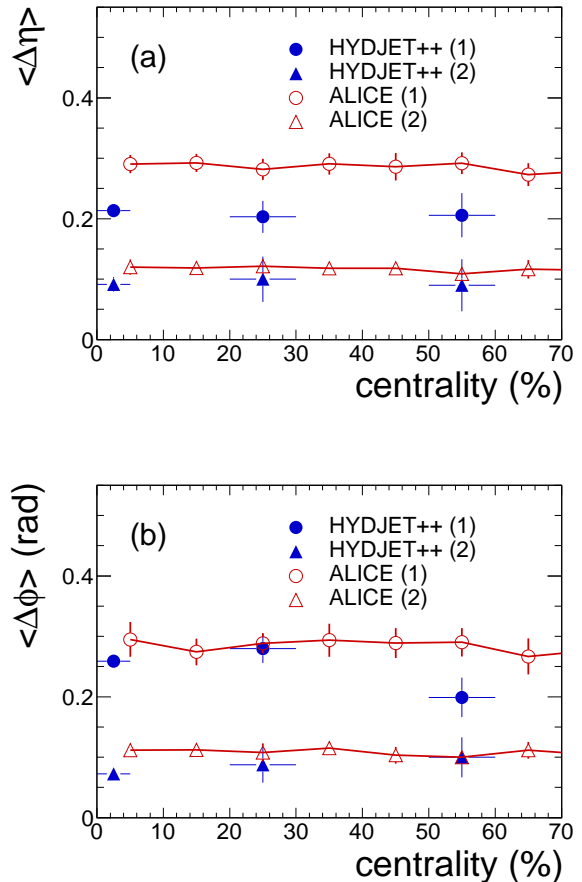


FIG. 4. (Color online) The same as Fig. 2 but for two transverse momentum intervals labeled in the text as (1) and (2). For the interval (1) HYDJET++ calculations and the data from [21] are denoted as full and open circles, respectively, whereas for the interval (2) the calculations and the data are indicated as full and open triangles. Lines are drawn to guide the eye.

majority of soft particles are generated within the statistical model approach independently, and the charge correlations emerge merely as a result of the resonance decays. The widths $\langle\Delta\eta\rangle_{\text{res}}$ are larger than $\langle\Delta\eta\rangle_{\text{exp}}$ and in accordance with the consideration above another source of the charge correlation with the width less than $\langle\Delta\eta\rangle_{\text{res}}$ should be implemented to provide the experimentally observed one in the considered interval of relatively low p_T .

In order to take the exact charge conservation into account we modified the generation procedure of soft direct hadrons. In the default model version a number N of particles with specified coordinates and momenta are generated in each event. In the modified version the following procedure is realized. For the sake of simplicity, we consider here the electrically neutral system similar to the midrapidity part of the fireball produced in heavy-ion collisions at LHC energies. Firstly, half of all charged particles is removed randomly in every event, whereas all

neutral particles remain unaffected. Then, for each particle with a given charge an antiparticle with an opposite charge is added to the particle spectrum. For instance, π^- should be added to π^+ , and vice versa. The coordinates and the transverse momenta of new particles are ascribed as the same as one of the corresponding original particles, providing the charge conservation locally. The pseudorapidities and the azimuthal angles of these new particles are distributed around the pseudorapidities and the azimuthal angles of corresponding original particles. The Gaussian distributions are used

$$P(x) = \frac{1}{\sqrt{2\pi}\sigma_x} \times \exp \left[-\frac{(x - x_0)^2}{2\sigma_x^2} \right]$$

Here $x = \{\eta; \varphi\}$, and dispersions σ_x of the distributions are new parameters of the model. They should provide the widths of the charge balance function less than $\langle \Delta\eta \rangle_{\text{res}}$ and $\langle \Delta\varphi \rangle_{\text{res}}$ to reproduce the experimental data in the most central collisions. As a result, the equal number of particles with positive and negative charges will be obtained in each newly generated event. - As a matter of fact, the pairs of particles and antiparticles correlated in the pseudorapidity and the azimuthal angle are generated in a similar way in other models. - Finally, the spectra of newly generated direct hadrons remain almost unchanged, but their balance function will be nonzero with a some finite width, in contrast to the original procedure with the formally infinite width of soft direct hadrons, because we have no charge correlations at all due to the independent generation of particles. The dispersion of Gaussian distributions should be fitted to reproduce the centrality dependence of widths in the intervals of relatively low transverse momenta.

The results of our fitting procedure are shown in Fig. 5. The model calculations reproduce the experimentally observed centrality dependence of widths rather well if the dispersions of Gaussian distributions increase with the growth of the impact parameter. This indicates that the charge correlations of direct hadrons become weaker in more peripheral collisions compared with central ones. Indeed the number of the characteristic elementary volumes, i.e., the independent particle sources, in which the charge is explicitly conserved, decreases with the growth of the impact parameter since the area of the nuclear overlap region becomes smaller. It means that the fluctuations become stronger [44], thus reducing the charge correlation in general. Here it is worth mentioning the recently developed method [45] to ensure conservation laws for each sampled configuration in spatially compact regions, or patches, at the freeze-out stage. This method allows one also to study the correlation effects sensitive to the patch size as a fitting parameter. Our procedure is considerably simpler for the realization in Monte Carlo event generators and does not imply any modification of single particle spectra and any additional tuning of other free parameters of the model.

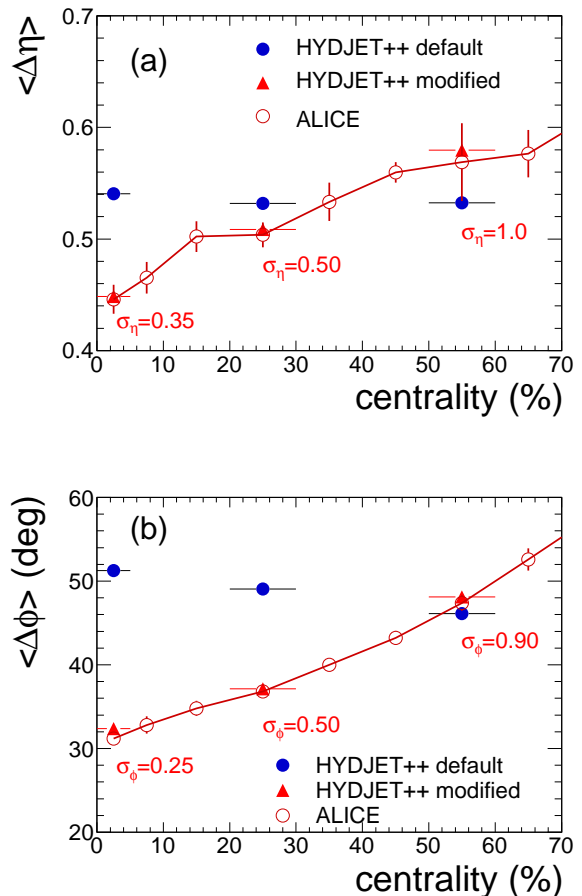


FIG. 5. (Color online) The same as Fig. 2 but for calculations with modified version of HYDJET++ (triangles) in which the exact charge conservation is taken into account. Full circles denote the default version calculations and open circles indicate the experimental data. Lines are drawn to guide the eye.

V. CONCLUSIONS

The phenomenological analysis of charge balance function in Pb+Pb collisions at center-of-mass energy 2.76 TeV per nucleon pair has been performed within the two-component HYDJET++ model. It is shown that the experimentally observed increase of the balance function width with increasing impact parameter at relatively low transverse momentum interval can be qualitatively reproduced by the relative enhancement of the contribution from the hard component in peripheral Pb+Pb collisions. However, the centrality dependence of the CBF magnitude shows opposite tendency compared to the experimental one. The fully adequate description of the balance function in this interval assumes the essential model modification by means of inclusion of the charge conservation explicitly in a statistical approach. This procedure has been implemented for the first time in Monte Carlo

event generators of a such kind. With increasing transverse momentum the default model results describe experimental data much better, because in these transverse momentum intervals the contribution from the soft component of the model is weakened. Practically, we observe the transition to the single source of charge correlations, namely, the charge correlations in jets for which the exact

charge conservation takes place at each stage.

ACKNOWLEDGMENTS

Fruitful discussions with A.V. Belyaev, L.V. Bravina and A.I. Demyanov are gratefully acknowledged.

-
- [1] *Proceedings of Quark Matter 2019*, edited by F. Liu, E. Wang, X.-N. Wang, N. Xu and B.-W. Zhang, Nucl. Phys. A **1005**, 122104 (2021).
- [2] *Proceedings of Quark Matter 2018*, edited by F. Antinori, A. Dainese, P. Giubellino, V. Greco, M.P. Lombardi, and E. Scapparini, Nucl. Phys. A **982**, 1-1066 (2019).
- [3] I.P. Lokhtin, L.V. Malinina, S.V. Petrushanko, A.M. Snigirev, I. Arsene, and K. Tywoniuk, Comput. Phys. Commun. **180**, 779 (2009).
- [4] I.P. Lokhtin, A.V. Belyaev, L.V. Malinina, S.V. Petrushanko, E.P. Rogochaya, and A.M. Snigirev, Eur. Phys. J. C **72**, 2045 (2012).
- [5] L.V. Bravina, B.H. Brushheim Johansson, G.Kh. Eyyubova, V.L. Korotkikh, I.P. Lokhtin, L.V. Malinina, S.V. Petrushanko, A.M. Snigirev, and E.E. Zabrodin, Eur. Phys. J. C **74**, 2807 (2014).
- [6] L.V. Bravina, E.S. Fotina, V.L. Korotkikh, I.P. Lokhtin, L.V. Malinina, E.N. Nazarova, S.V. Petrushanko, A.M. Snigirev, and E.E. Zabrodin, Eur. Phys. J. C **75**, 588 (2015).
- [7] I.P. Lokhtin, A.V. Belyaev, and A.M. Snigirev, Eur. Phys. J. C **71**, 1650 (2011).
- [8] I.P. Lokhtin, A.A. Alkin, and A.M. Snigirev, Eur. Phys. J. C **75**, 452 (2015).
- [9] G. Eyyubova, V.L. Korotkikh, I.P. Lokhtin, S.V. Petrushanko, A.M. Snigirev, L.V. Bravina, and E.E. Zabrodin, Phys. Rev. C **91**, 064907 (2015).
- [10] S.A. Bass, P. Danielewicz, and S. Pratt, Phys. Rev. Lett. **85**, 2689 (2000).
- [11] S. Jeon and S. Pratt, Phys. Rev. C **65**, 044902 (2002).
- [12] S. Pratt and C. Plumberg, Phys. Rev. C **104**, 014906 (2021).
- [13] B. Ling, T. Springer, and M. Stephanov, Phys. Rev. C **89**, 064901 (2014).
- [14] W. Florkowski, W. Broniowski, and P. Bozek, J. Phys. G **30**, S1321 (2004).
- [15] A. Bialas, Phys. Lett. B **579**, 31 (2004).
- [16] S. Cheng, S. Petriconi, S. Pratt, M. Skoby, C. Gale, S. Jeon, V. Topor Popp, and Q.-H. Zhang, Phys. Rev. C **69**, 054906 (2004).
- [17] J. Adams *et al.* (STAR Collaboration), Phys. Rev. Lett. **90**, 172301 (2003).
- [18] M.M. Aggarwal *et al.* (STAR Collaboration), Phys. Rev. C **82**, 024905 (2010).
- [19] L. Adamczyk *et al.* (STAR Collaboration), Phys. Rev. C **94**, 024909 (2016).
- [20] J. Adam *et al.* (ALICE Collaboration), Eur. Phys. J. C **76**, 86 (2016).
- [21] B. Abelev *et al.* (ALICE Collaboration), Phys. Lett. B **723**, 267 (2013).
- [22] J. Pan, Nucl. Phys. A **982**, 315 (2019).
- [23] A. Tawfik and A.G. Shalaby, Adv. High Energy Phys. **2015**, 186812 (2015).
- [24] M. Gyulassy and X.-N. Wang, Comput. Phys. Commun. **83**, 307 (1994).
- [25] M. Gyulassy and X.-N. Wang, Phys. Rev. D **44**, 3501 (1991).
- [26] B. Zhang, C.M. Ko, B.-A. Li, and Z.W. Lin, Phys. Rev. C **61**, 067901 (2000).
- [27] Z.W. Lin, S. Pal, C.M. Ko, B.-A. Li, and B. Zhang, Phys. Rev. C **64**, 011902 (2001).
- [28] Z.W. Lin, C.M. Ko, B.-A. Li, B. Zhang, and S. Pal, Phys. Rev. C **72**, 064901 (2005).
- [29] T. Pierog, Iu. Karpenko, J.M. Katzy, E. Yatsenko, and K. Werner, Phys. Rev. C **92**, 034906 (2015).
- [30] S. Ostapchenko, Phys. Rev. D **83**, 014018 (2011).
- [31] B.-H. Sa, D.-M. Zhou, Y.-Li. Yan, X.-M. Li, S.-Q. Feng, B.-G. Dong, and X. Cai, Comput. Phys. Commun. **183**, 333 (2012).
- [32] Z.-L. She, D.-M. Zhou, Y.-L. Yan, L. Zheng, H.-G. Xu, G. Chen, and B.-H. Sa, Comput. Phys. Commun. **274**, 108289 (2022).
- [33] C. Bierlich, G. Gustafson, L. Lönnblad, and H. Shah, JHEP **10**, 134 (2018).
- [34] L.V. Bravina, G.Kh. Eyyubova, V.L. Korotkikh, I.P. Lokhtin, S.V. Petrushanko, A.M. Snigirev, and E.E. Zabrodin, Phys. Rev. C **103**, 034905 (2021).
- [35] A.M. Sirunyan *et al.* (CMS Collaboration), Phys. Lett. B **776**, 195 (2018).
- [36] N.S. Amelin, R. Lednicky, T.A. Pocheptsov, I.P. Lokhtin, L.V. Malinina, A.M. Snigirev, Iu.A. Karpenko, and Yu.M. Sinyukov, Phys. Rev. C **74**, 064901 (2006).
- [37] N.S. Amelin, R. Lednicky, I.P. Lokhtin, L.V. Malinina, A.M. Snigirev, Iu.A. Karpenko, Yu.M. Sinyukov, I. Arsene, and L. Bravina, Phys. Rev. C **77**, 014903 (2008).
- [38] I.P. Lokhtin and A.M. Snigirev, Eur. Phys. J. C **45**, 211 (2006).
- [39] U. Wiedemann, Phys. Rev. C **57**, 266 (1998).
- [40] J. Crkovska, J. Bielcik, L. Bravina, B.H. Brushheim Johansson, E. Zabrodin, G. Eyyubova, V.L. Korotkikh, I.P. Lokhtin, L.V. Malinina, S.V. Petrushanko, and A.M. Snigirev, Phys. Rev. C **95**, 014910 (2017).
- [41] L.V. Bravina, I.P. Lokhtin, L.V. Malinina, S.V. Petrushanko, A.M. Snigirev, and E.E. Zabrodin, Eur. Phys. J. A **53**, 219 (2017).
- [42] HYDJET++ 2.4, <https://lokhtin.web.cern.ch/lokhtin/hydjet++/>
- [43] J. Fu, J. Phys. G **38**, 065104 (2011).
- [44] G. Eyyubova, V.L. Korotkikh, A.M. Snigirev, and E.E. Zabrodin, J. Phys. G **48**, 095101 (2021).
- [45] D. Oliinychenko, S. Shi, and V. Koch, Phys. Rev. C **102**, 034904 (2020).